Available online at www.sciencedirect.com

SCIENCE DIRECT®

Ecological Modelling 170 (2003) 407–426

ECOLOGICAL MODELLING

www.elsevier.com/locate/ecolmodel

Canopy structure versus physiology effects on net photosynthesis of mountain grasslands differing in land use☆

Georg Wohlfahrt[a,*], Michael Bahn[a], Christian Newesely[a], Sigrid Sapinsky[a], Ulrike Tappeiner[a,b], Alexander Cernusca[a]

[a] *Institut für Botanik, Universität Innsbruck, Sternwartestraße. 15, 6020 Innsbruck, Austria*
[b] *Europäische Akademie Bozen, Domplatz 3, Bozen, 39100 Bolzano, Italy*

Abstract

The present paper aims at investigating how changes in canopy structure and species physiology associated with the abandonment of mountain meadows and pastures affect their net photosynthesis. For this purpose, a multi-layer vegetation–atmosphere transfer (VAT) model is employed, which explicitly takes into account the structural and functional properties of the various canopy components and species. Three sites differing in land use are investigated, a meadow, a pasture and an abandoned area. Model simulations agree reasonably with measured canopy net photosynthetic rates, the meadow featuring the highest daily net photosynthesis, followed by the pasture and, finally, the abandoned area. A detailed process analysis suggests this ranking to be mainly due to bulk canopy physiology, which decreases from the meadow to the pasture and the abandoned area, reflecting species composition and species-specific photosynthetic capacities. Differences between the canopies with regard to canopy structure are found to be of minor importance. The amounts of green, photosynthetically active plant matter are too similar at the three sites to be a major source of variation in net photosynthesis. Large differences exist between the canopies with regard to the amount of photosynthetically inactive phytoelements. Even though a model analysis showed them to be potentially important, most of them are accumulated close to the ground surface, where they exert little influence on canopy net photosynthesis.

Keywords: Abandonment; Canopy structure; Dead plant matter; Meadow; Pasture; Photosynthesis; Radiation absorption

1. Introduction

The global rise in atmospheric CO_2 concentrations and the expected negative consequences therefrom, have increased, at least in the scientific community, the awareness about the role of terrestrial ecosystems in the biosphere–atmosphere exchange of CO_2 (e.g. Steffen et al., 1998; Lloyd, 1999; Smith et al., 2000; Valentini et al., 2000). Land-use changes play an important role in this context, since they have the potential to modify ecosystem source/sink relationships, which in turn will feed back on atmospheric CO_2 concentrations (Houghton, 1995, 1999; IPCC, 2000).

Mountain grassland farming in the Alps is undergoing major changes with regard to land use (Cernusca et al., 1992, 1996, 1998a,b, 1999). Created centuries ago by cutting the predominating mixed evergreen/deciduous forests, these grasslands have been kept in an ecological balance by traditional human management practices, i.e. hay making and graz-

☆ Special issue on the 3rd conference of the European chapter of the *International Society of Ecological Modelling*.

* Corresponding author. Tel.: +43-512-507-5917; fax: +43-512-507-2715.
E-mail address: Georg.Wohlfahrt@uibk.ac.at (G. Wohlfahrt).

0304-3800/$ – see front matter © 2003 Elsevier B.V. All rights reserved.
doi:10.1016/S0304-3800(03)00242-4

ing by domestic ungulates. During the last decades, however, fundamental socio-economic changes have triggered the abandonment of a rapidly increasing part of this formerly intensively managed grassland, opening these areas to secondary succession by re-colonising shrub and tree species (Paldele, 1994). These transformations affect the spatial structure of plant canopies (Tappeiner and Cernusca, 1994, 1996, 1998a,b; Rosset et al., 1999), species composition (Spatz et al., 1993; Tasser et al., 1999) and physiology (Cernusca et al., 1992; Tappeiner and Cernusca, 1998a; Bahn et al., 1999; Wohlfahrt et al., 1999a), and in consequence canopy net photosynthetic rates.

Previous comparisons of mountain grasslands differing in land use showed that abandonment of meadows and pastures results in a reduction of canopy net photosynthesis compared to their managed state (Tappeiner and Cernusca, 1996, 1998a,b; Tappeiner et al., 1999b). Attempts to explain the observed decrease of net photosynthesis in abandoned areas may be classified into two broad groups, (I) those centred on the effects of canopy structure, and (II) those emphasising the role of species physiology, as detailed below:

(I) A characteristic feature of abandoned mountain grasslands is the accumulation of dead, photosynthetically inactive plant matter (Cernusca et al., 1992; Tappeiner and Cernusca, 1994, 1996, 1998b; Rosset et al., 1999). Meadows and pastures typically comprise much smaller fractions of dead plant matter (Cernusca et al., 1992; Tappeiner and Cernusca, 1994, 1996, 1998b), being kept in a stage of continuing growth by cutting and grazing, respectively (Fox et al., 1998; Lentz and Cipollini, 1998). Absorption of photosynthetically active radiation (PPFD) supplies the energy required for CO_2 assimilation by green plants. Photosynthetically inactive phytoelements, however, also absorb PPFD, but do not contribute to net photosynthesis. The higher net photosynthetic rates of meadows and pastures may thus be attributed to the fact that less PPFD is 'lost' to photosynthetically inactive canopy components, compared to abandoned areas, but remains available to the photosynthetically active ones, which allows for higher net photosynthetic rates.

(II) Carbon uptake by the canopy as a whole depends on the photosynthetic potential of the species making up the canopy and the prevailing environmental forcing variables, which set limits to the extent to which the species are able to realise their potential (Beyschlag et al., 1990; Baldocchi and Harley, 1995; Leuning et al., 1995). The observed differences in canopy net photosynthesis may hence result from the lower bulk photosynthetic capacity of abandoned areas, as compared to meadows and pastures. The reason for this is two-fold: first, species typical of abandoned areas, such as dwarf shrubs or the bunch grass *Nardus stricta*, have comparably lower photosynthetic capacities as compared to species typically found at meadows and pastures (Cernusca et al., 1992; Bahn et al., 1999). In addition, abandonment is accompanied by a reduction in nitrogen availability (Zeller et al., 2000), causing leaf nitrogen contents to decrease with respect to meadows and pastures (Bahn et al., 1994, 1999; Wohlfahrt et al., 1999a). Since photosynthetic capacity is tightly correlated to leaf nitrogen content (e.g. Field and Mooney, 1986; Evans, 1989; Reich et al., 1995; Bahn et al., 1999), a decrease in photosynthetic performance is the consequence.

Drawing upon field measurements conducted within the EU-TERI project ECOMONT (Cernusca et al., 1996, 1998a,b, 1999), it is the aim of the present paper to examine how canopy structure and species physiology affect canopy net photosynthesis in order to assess the validity of the aforementioned hypothesis for explaining the observed differences in canopy net photosynthesis. Since the complexity of the underlying processes precludes this topic from being analysed solely on the basis of experimental data, a vegetation–atmosphere transfer (VAT) model (Wohlfahrt et al., 1998, 2000, 2001) will be employed. Parameterised with site-specific data, simulations with the VAT-model will be conducted for a meadow, a pasture and an abandoned area from three ECOMONT study areas in the Eastern Alps. In a first step, simulation results will be validated against CO_2 exchange measurements made in the field, subsequently model results will be evaluated with regard to the hypothesised relationships.

2. Material and methods

2.1. Site

Field investigations were carried out during the summers of 1996–1998 at three study areas, Stubai Valley, Passeier Valley and Monte Bondone, situated along a north–south transect across the Eastern Alps. The study areas are situated along an altitudinal gradient, the southern-most study area (Monte Bondone) at the lowest elevation and the northern-most (Stubai Valley) at the highest (Table 1). Average air temperatures at the study areas decrease along the north–south transect (Table 1). Average annual precipitation (Table 1) is similar in Stubai and Passeier Valley, whereas the higher precipitation at the Monte Bondone study area reflects its location at the southern border of the Alps, being influenced by both the Mediterranean and the continental climate.

At each study area a differently managed study site was selected in order to provide a representative range of grassland ecosystems from the Eastern Alps: a pasture, grazed by cattle from early summer till autumn, was studied at Stubai Valley (Bitterlich and Cernusca, 1999). At Passeier Valley (Tappeiner et al., 1999a) a former hay meadow, abandoned approximately 10 years ago, was selected. A hay meadow, mowed once a year by the end of July, was investigated at Monte Bondone (Cescatti et al., 1999). The plant area index (PAI, m^2 plant area per m^2 ground area) decreases from the abandoned area (5.5), to the meadow (4.8) and the pasture (3.7), as shown in Table 1. The ratio between photosynthetically active and inactive phytoelements (Table 1) is highest at the pasture (4.3) and similarly low at the meadow (1.4) and the abandoned area (1.0). At the meadow this is caused by the accumulation of dead plant material (37.1%) close to the soil surface (Fig. 1), whereas at the abandoned area

Table 1
General characterisation of the three study sites

	Monte Bondone	Stubai Valley	Passeier Valley
Latitude	46°01′	47°07′	46°50′
Longitude	11°02′	11°17′	11°17′
Altitude (m a.s.l.)	1565	1950 (1750[a])	1770 (1618[a])
Average annual rainfall (mm)	1189	1097	1041
Average annual air temperature (°C)	5.5	3.0	3.6
Land use	Meadow	Pasture	Abandoned
Soil type	Cambisol	Cambisol	Cambisol
Vegetation type	Arrhenateretum elatioris	Alchemillo Poetum supinae	Caricetum sempervirentis
Maximum canopy height (m)[b]	0.64	0.24	0.24
Plant area index ($m^2\,m^{-2}$)[b,c]	4.8	3.7	5.5
Green area index ($m^2\,m^{-2}$)[b,c]	2.8	3.0	2.7
Average phytoelement inclination angle (°)	50	46	60
Plant components[d]			
Reproductive organs	4.2	1.8	1.4
Attached dead plant matter	37.1	17.2	34.5
Cryptogams	1.1	–	1.3
Forb stems	5.3	6.1	2.1
Graminoid stems	11.6	1.2	1.4
Dwarf shrub stems	–	–	14.1
Forb leaves	15.9	43.4	13.1
Graminoid leaves	24.8	30.3	3.3
Dwarf shrub leaves	–	–	28.8

[a] Altitude of meteorological station, if different from that of the study area.
[b] By the end of July.
[c] On a hemi-surface area basis.
[d] Percentage of total PAI.

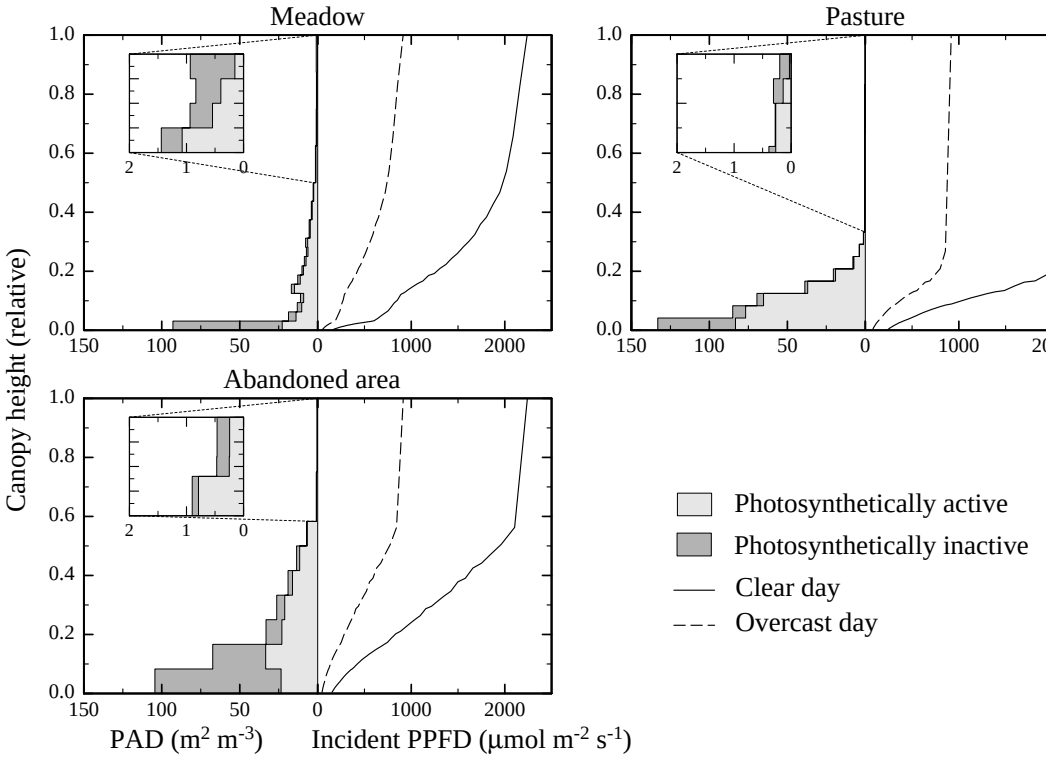

Fig. 1. Vertical distribution of the plant area density (PAD), separately for photosynthetically active and inactive phytoelements, and simulated penetration of PPFD at noon (12:00 h CET) for the clear and overcast day scenario. Plant area densities in the upper canopy layers have been enlarged in the insets for clarity.

the reason is both the large proportion of dead plant material (34.5%), as well as the presence of photosynthetically inactive supporting structures of dwarf shrub species, the latter amounting at 14.1% (Table 1). Plant area density (m^2 plant area per m^3 occupied volume) increases gently towards the ground (except for the lowermost canopy layer) at the meadow, whereas almost all of the phytomass is concentrated below a relative canopy height of 0.3 (=0.08 m) at the pasture (Fig. 1). The vertical structure of the abandoned area resembles the pasture, except for the increase in plant area density with decreasing canopy height commencing at a relative canopy height of 0.6 (=0.14 m) and not being as extreme as at the pasture (Fig. 1).

2.2. Experimental methods

Leaf gas exchange measurements were carried out on the most abundant species as described previously in detail by Wohlfahrt et al. (1998, 1999a), and are thus not repeated. A detailed description of the methods of measuring the microclimate and the fluxes of CO_2 and energy may be found in Tappeiner et al. (1999b). Briefly, measurement were made using the battery-powered data acquisition system MIKROMET (Cernusca, 1987) at intervals ranging from 1 to 6 min, from which hourly mean values were calculated. Incoming short-wave radiation was measured using two star pyranometers, net radiation by the means of net radiometers (Schenk, Vienna, Austria). Soil temperatures (0, 0.05, 0.1, 0.2, and 0.5 m) and air temperatures within the canopy were measured using thermocouples (copper/constantan, 8×10^{-5} m diameter). CO_2 concentrations were measured using an infrared gas analyser (CIRAS-Sc, PP-Systems, Hitchin Herts, UK), water vapour pressure by the means of thermocouple psychrometers, both at 0.1 and 0.7 m above the canopy, and 2 m above ground. The energy balance

and the flux of CO_2 above the canopy were calculated by the Bowen ratio energy balance (BREB) method (Perez et al., 1999). Positive flux densities represent mass and energy transfer directed away from the soil surface, negative values denote the reverse. Soil heat flux was estimated by a combination of the temperature integral method for the upper 0.2 m of the soil and the temperature gradient method for the lower layers of the soil. CO_2 release from the soil (R_{soil}) was measured in situ by IRGA techniques. Canopy net photosynthesis (A_C) was then calculated as $F_C + R_{soil}$, where F_C is the CO_2 flux above the canopy (all $\mu mol\, m^{-2}\, s^{-1}$).

Canopy structure was assessed by the end of July, before the meadow was cut, by stratified clipping of plots of 0.3–0.5 m side length. Thickness of the harvested layers ranged between 0.01 and 0.04 m. Silhouette area was determined by the means of an area meter (Li-3100, Li-Cor, Lincoln, USA). The harvested plant material was separated as follows: leaves were separated into those species that had the largest fractional contribution to total PAI. Six species were identified at the abandoned area (*Arnica Montana* L., *Calluna vulgaris* (L.) Hull, *N. stricta* L., *Potentilla aurea* Torn., *Trifolium repens* L., *Vaccinium myrtillus* L.), five at the meadow (*Achillea millefolium* L., *Rhinanthus alectorolophus* (Scop.) Poll., *Rumex arifolius* All., *T. pratense* L., *Trollius europaeus* L.), and four at the pasture (*Alchemilla vulgaris* L., *N. stricta* L., *Plantago media* L., *T. montanum* L.). In the following the first letter of the generic name together with the full species name will be used to abbreviate species names unless otherwise indicated. The remaining leaves were pooled to two functional groups: forbs and graminoids. Separation into these functional groups was also made for stems of forbs and graminoids; for dwarf shrubs, present only at the abandoned area, distinction was made between green and non-green woody stems. The remaining plant components, i.e. reproductive organs, attached dead plant matter and cryptogams, were pooled over all species. Phytoelement inclinations and widths were measured in the field with a hand inclinometer with a five degrees accuracy and a ruler, respectively.

2.3. Models

In the present study, a one-dimensional, multi-layer model is used to compute the steady-state fluxes of CO_2 (and energy, the latter though being out of the scope of the present article) between the vegetation and the atmosphere. The model consists of micrometeorological and physiological modules: the environmental variables computed in the micrometeorological modules represent the driving forces for the energy balance model, which partitions absorbed energy into emitted long-wave radiation, metabolic storage, latent and sensible heat fluxes. Net photosynthesis, respiration, and stomatal conductance are calculated in a sub-module of the energy balance model, whenever applicable.

The phytoelements making up the canopy are separated into one of three physiological categories (cf. Wohlfahrt et al., 2001). Phytoelements, such as leaves, green stems of herbaceous species and cryptogams, able to assimilate CO_2, belong to the first category. The second category covers the canopy components characterised by a positive CO_2 balance (i.e. respiration), such as non-green and green woody stems of dwarf shrubs (Siegwolf, 1987). The third category comprises all phytoelements with zero CO_2 gas exchange. Attached dead plant material is assigned to the last category, thereby neglecting CO_2 loss resulting from microbial decay.

A short description of the model theory is given in Appendix A, for details we refer to our previous papers (Wohlfahrt et al., 1998, 2000, 2001).

2.4. Meteorological driving forces

The present analysis is based upon simulations conducted for two contrasting weather scenarios, a clear and an overcast day, as they are typical for the end of July, the peak season. The fact that we are comparing three sites, which are characterised by differing climatic conditions (Table 1), poses some practical problems for the present study, since differences with regard to canopy net photosynthesis may not be exclusively due to land use, but also due to differing climatic conditions. In order to be able to clearly separate land-use-related from site-specific climatic effects, we have thus decided to use the same, average meteorological driving forces for all three sites (Fig. 2). The consequences of this ‘abstraction’, which neglects site-specific climatic phenomena and the feedback influence of vegetation on local climatic conditions, was assessed by a comparison with canopy net photosyn-

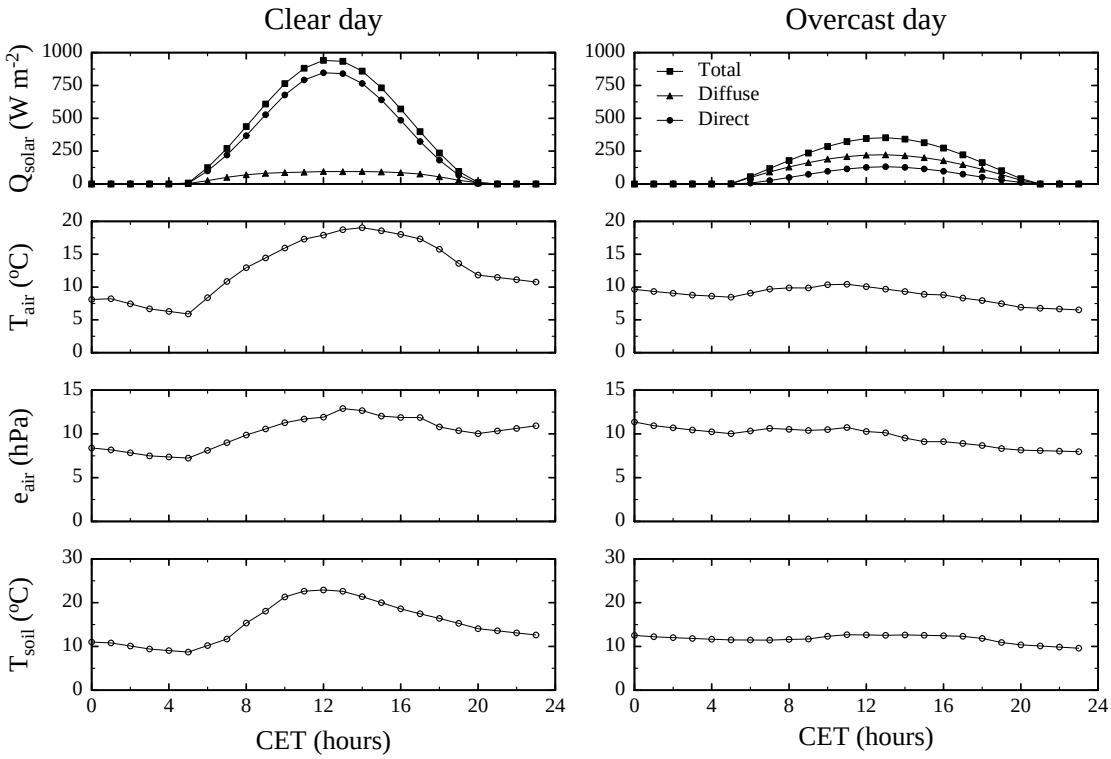

Fig. 2. Environmental forcing variables supplied to the model as input parameters (Q_{solar}, short-wave radiation; T_{air}, air temperature at 2 m; e_{air}, air vapour pressure at 2 m; T_{soil}, soil surface temperature). Short-wave radiation is further separated into its direct and diffuse component. Wind speed (at 2 m) was set to a constant, average value of 2 m s^{-1} both for the clear and overcast day scenario, CO_2 partial pressures were assumed to be constant at 340 and 350 μmol mol^{-1} for the clear and overcast day scenario, respectively.

thetic rates calculated on the basis of site-specific climatic conditions. The choice of the meteorological driving forces (average or site-specific) did not affect results for the clear day scenario, but for overcast conditions, when differences between the sites were larger, somewhat changed the relative differences between the sites, albeit without altering the overall trend. For the purpose of the present paper, we thus conclude that using average meteorological driving forces is justified. Validation (Fig. 3) is of course based on the actual meteorological driving forces.

3. Results

3.1. Validation

Fig. 3 shows the bin averaged, diurnal variation of observed and predicted net photosynthesis of the three investigated canopies. Note that due to the fact that the BREB-technique does not allow reliable (CO_2) exchange measurements to be made during periods of small scalar gradients and/or available energy (Perez et al., 1999), no comparison between measured and simulated night-time CO_2 exchange can be made. Simulations compare favourably with measured daytime net photosynthesis insofar that they reasonably capture the observed diurnal patterns (Fig. 3). As evident from the slope and *y*-intercept of a linear regression analysis (Table 2), there is a trend of overestimating daytime net photosynthesis at the meadow, whereas the reverse is true for the pasture and the abandoned area. The mean error (Table 2) is close to zero for the pasture and abandoned area, and amounts at -2.10 μmol m^{-2} s^{-1} for the meadow. Overall, model calculations account for at least 95% of the variance in measurements (Table 2).

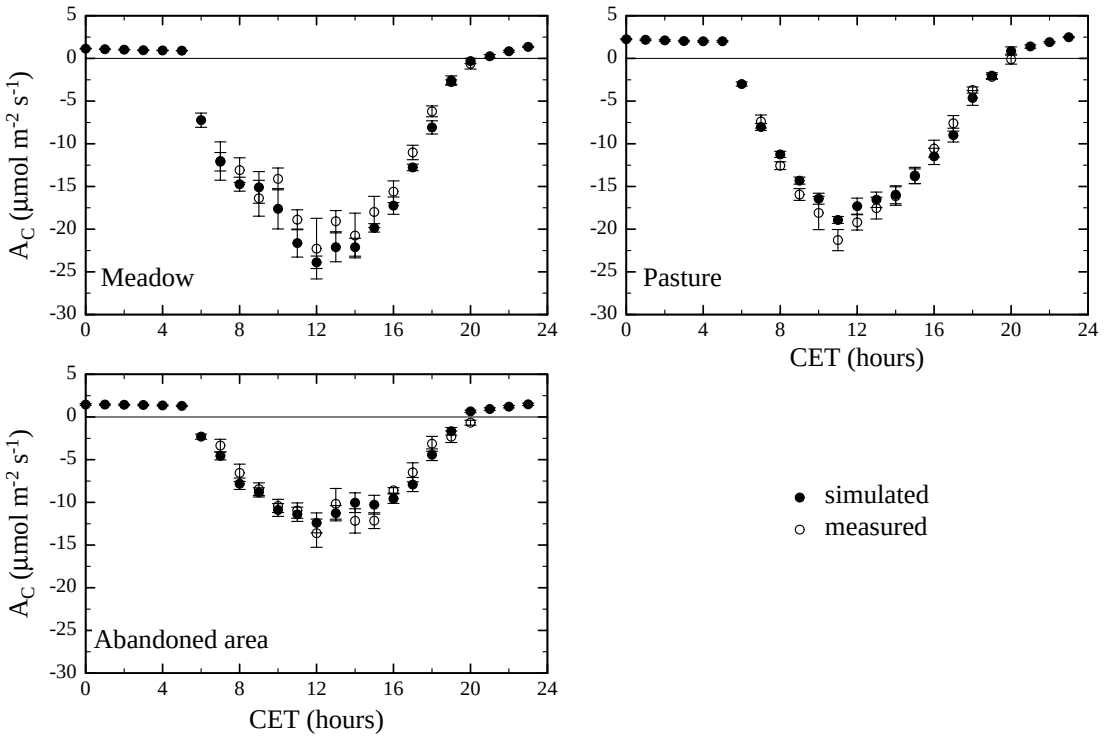

Fig. 3. Bin averaged, diurnal course of measured and simulated canopy net photosynthesis of the three sites. Error bars represent 1 standard deviation.

3.2. Canopy structure and radiation absorption

Fig. 4 shows how the differences in PAI (Table 1) and canopy structure (Fig. 1) are reflected in the absorption of PPFD. At the pasture more than 80% of the incoming PPFD is absorbed by photosynthetically active and only about 7% by photosynthetically inactive canopy components. At the meadow and the abandoned area the proportion of PPFD absorbed by photosynthetically active phytoelements is smaller, 70 and 73%, respectively (Fig. 4), whereas PPFD absorbed by photosynthetically inactive phytoelements amounts at 21 and 18%, respectively. Note the comparably larger amount of radiation being absorbed by the soil of the pasture, bearing prominent implications for the surface energy balance (cf. Tappeiner and Cernusca, 1994, 1998b).

Table 2
Statistics for comparison between measured and simulated net photosynthesis of the investigated canopies

Site	Slope	*y*-intercept	EV	MD
Meadow	1.02 ± 0.08	−1.84 ± 1.16	97	−2.10
Pasture	0.94 ± 0.02	−0.59 ± 0.25	98	0.04
Abandoned area	0.93 ± 0.06	−0.77 ± 0.49	95	−0.23

Model performance is evaluated by the slope and the *y*-intercept (μmol m^{-2} s^{-1}) of a linear regression (mean ± standard error), the explained variance, EV (%), and the mean difference between simulations and measurements, MD (μmol m^{-2} s^{-1}).

The amount of absorbed PPFD parallels the increase in plant area density with decreasing height to a point of inflection, where any further increase in plant area density is offset by the associated decrease in available radiation (Fig. 1), from where on it decreases (Fig. 4). Closer inspection of Fig. 4 reveals, that the large amount of radiation absorbed by photosynthetically inactive phytoelements at the meadow, as opposed to the abandoned area, is due to the comparably large amount of reproductive organs at the canopy top (Table 1), absorbing on average 9.6% (i.e. almost half of the total radiation absorbed by photosynthetically inactive phytoelements) of the

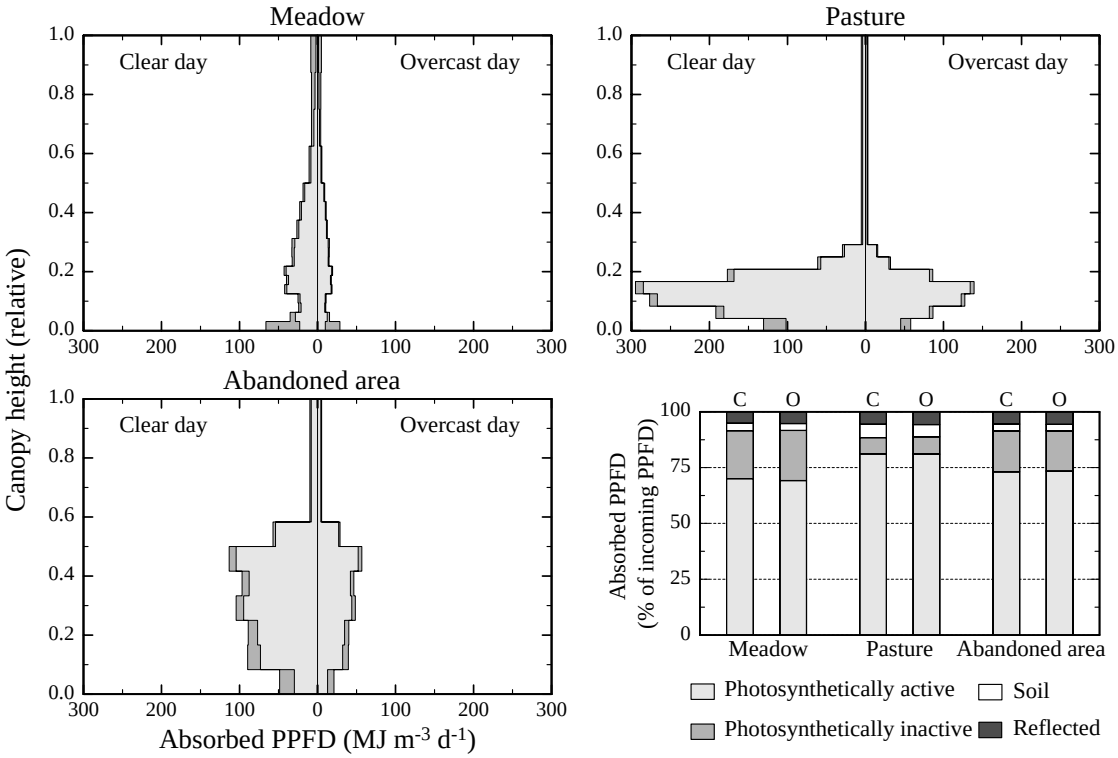

Fig. 4. Simulated vertical distribution of PPFD absorbed by photosynthetically active and inactive phytoelements and, lower right figure, simulated partitioning of PPFD into the proportions absorbed by photosynthetically active and inactive phytoelements, the soil and reflected back into the atmosphere. Simulations have been conducted for the clear (C) and overcast (O) day scenario.

incoming PPFD, but solely 1.5% at the abandoned area.

3.3. Species physiology and net photosynthesis

In order to assess the combined effects of species composition and species-specific differences in photosynthetic capacity on canopy net photosynthesis, a bulk photosynthetic capacity ($A_{C\,max}$) was defined, as

$$A_{C\,max} = \sum \mathrm{PAI}(i)^{-1} \left[\sum A_{max}(i)\,\mathrm{PAI}(i) \right], \qquad (1)$$

where $A_{max}(i)$ is the organ-level net CO_2 exchange rate of the ith component at a PPFD of 1500 μmol m^{-2} s^{-1}, an ambient CO_2 concentration of 350 μmol mol^{-1}, a leaf temperature of 20 °C and an air-to-leaf vapour pressure difference of 14 Pa kPa^{-1}. Note that in the case of the abandoned area, this quantity also comprises CO_2 losses by dwarf shrub bole respiration. The bulk photosynthetic capacity is highest for the meadow (13.4 μmol m^{-2} s^{-1}), followed by the pasture (10.5 μmol m^{-2} s^{-1}) and the abandoned area (5.6 μmol m^{-2} s^{-1}).

Net assimilation at the meadow and the pasture (Fig. 5) mimics the vertical profile of PPFD absorbed by photosynthetically active phytoelements (Fig. 4), reflecting the combined effects of the vertical distribution of green matter and PPFD availability (Fig. 1). This is true also for the abandoned area, except for the lower canopy layers, where respiration by dwarf shrub boles diminishes net photosynthesis, causing the daily CO_2 balance of the lowermost canopy layer to become even positive (Fig. 5). Total daily net photosynthesis is highest at the meadow, followed by the pasture and the abandoned area for the clear day scenario, but differences between the pasture and the abandoned area are narrowed during overcast conditions (Fig. 5).

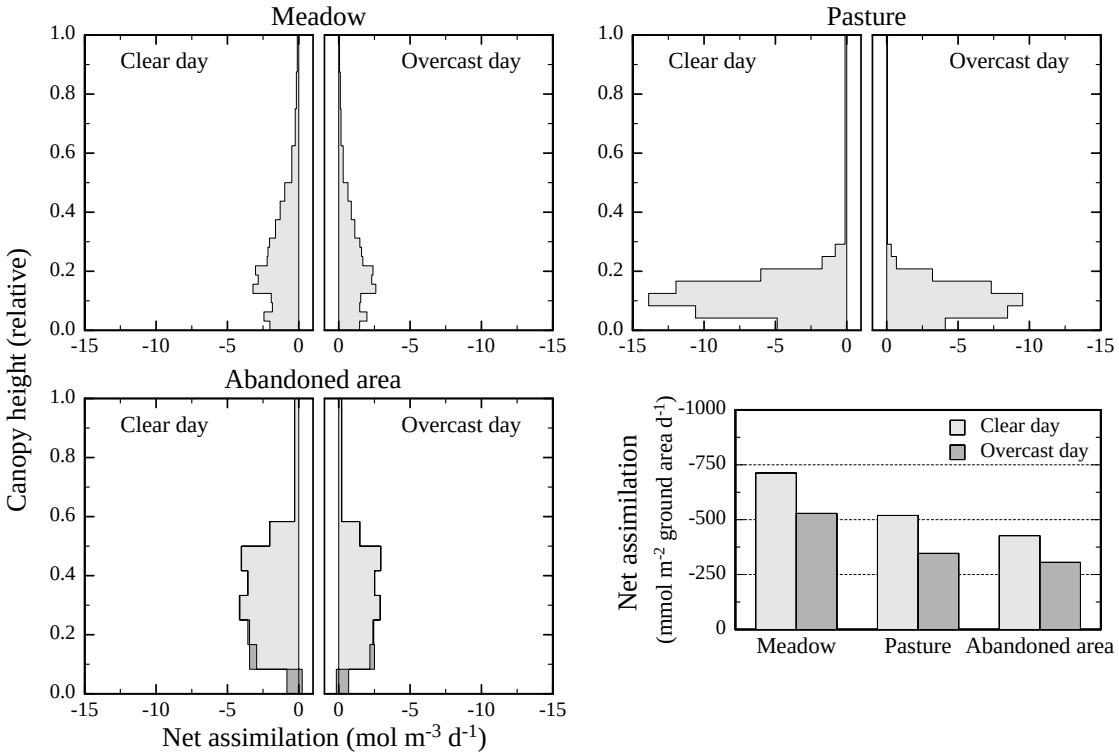

Fig. 5. Simulated vertical distribution of canopy net photosynthesis of the three sites for the clear and the overcast day scenario. In the case of the abandoned area (lower left figure), dark grey areas refer to CO_2 losses resulting from dwarf shrub bole respiration. The lower right figure shows total daily canopy net photosynthesis on a ground area basis.

3.4. Canopy structure and net photosynthesis

The previous analysis has been based on the actual green area indices (GAI) of the investigated canopies, which vary between 2.7 and 3.0 $m^2\,m^{-2}$ (Table 1). It is thus instructive to investigate how sensitive net photosynthesis is to variations in GAI, shown in Fig. 6. The potential impact of GAI on net photosynthesis is relatively small, varying by less than 8 and 10%, for clear (Fig. 6A) and overcast (Fig. 6B) sky conditions, respectively, for a 20% change in GAI. This is due to the fact that the actual green area indices are close to their optimum, which in turn is fairly broad.

The importance of the vertical distribution of the photosynthetically inactive phytomass for canopy net photosynthesis was assessed by two simulation experiments (Fig. 7). In the first one (Scenario I), we removed the dead plant material from the lowermost 2 and 4 cm of the meadow/pasture and the abandoned area, respectively. In the second experiment (Scenario II), we did the same, but redistributed the dead plant material uniformly in the upper canopy third. Removing all dead plant material from the lowermost canopy layers had almost no effect (±1%) on canopy net photosynthesis for clear sky conditions (Fig. 7), while a slight increase (1–4%) was observed for overcast conditions (data not shown). Redistributing the dead plant material to the upper canopy third reduced net photosynthesis by approximately 36 and 16% in the case of the meadow/abandoned area and the pasture, respectively, virtually irrespective of sky conditions (Fig. 7, data shown only for clear day). This reduction was due to lower maximum carbon uptake rates, as well as an extended period of CO_2 loss in the morning and evening (Fig. 7).

Finally, the role of canopy structure in determining net photosynthesis was tested by assigning the photosynthetically active phytoelements of all three

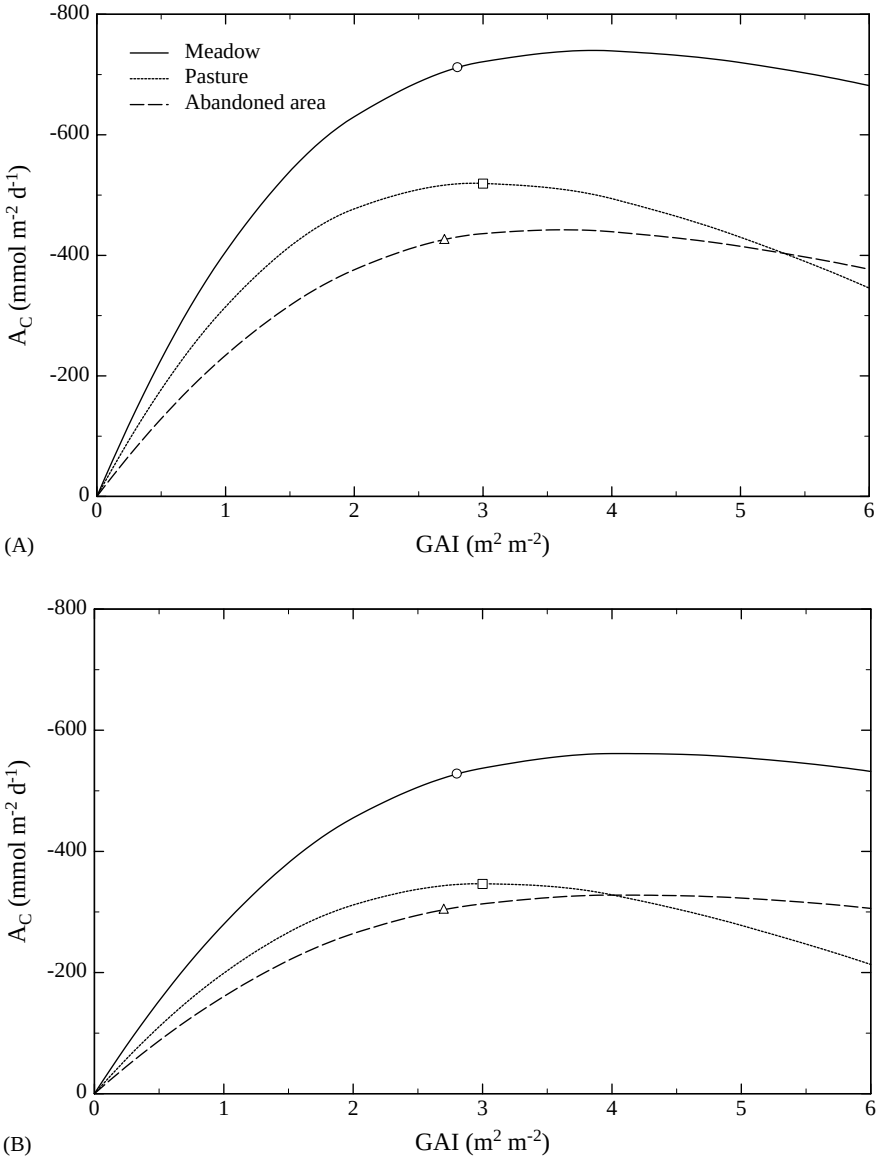

Fig. 6. Optimum green area indices for daily net photosynthesis of the investigated canopies for clear (A) and overcast (B) sky conditions. Symbols indicate net photosynthesis for the actual GAI of the investigated canopies. Green area indices were varied by proportional scaling of the total plant area indices, leaving all other parameters unchanged.

canopies the same physiological parameters. Under these circumstances, differences in net photosynthesis are attributable solely to canopy structure. As shown in the insets of Fig. 8, net photosynthesis is highest at the pasture, 2 and 6% lower at the meadow, and 15 and 16% lower at the abandoned area, for clear (Fig. 8A) and overcast (Fig. 8B) sky conditions, respectively. Thereby it is worth noting that the pasture, as compared to the meadow, compensates for lower maximum net photosynthetic rates during clear sky conditions by lower night-time respiration rates, as well as a higher light use efficiency in the morning/evening (Fig. 8A). Under overcast sky conditions, in contrast, net photosynthesis of the pastures exceeds

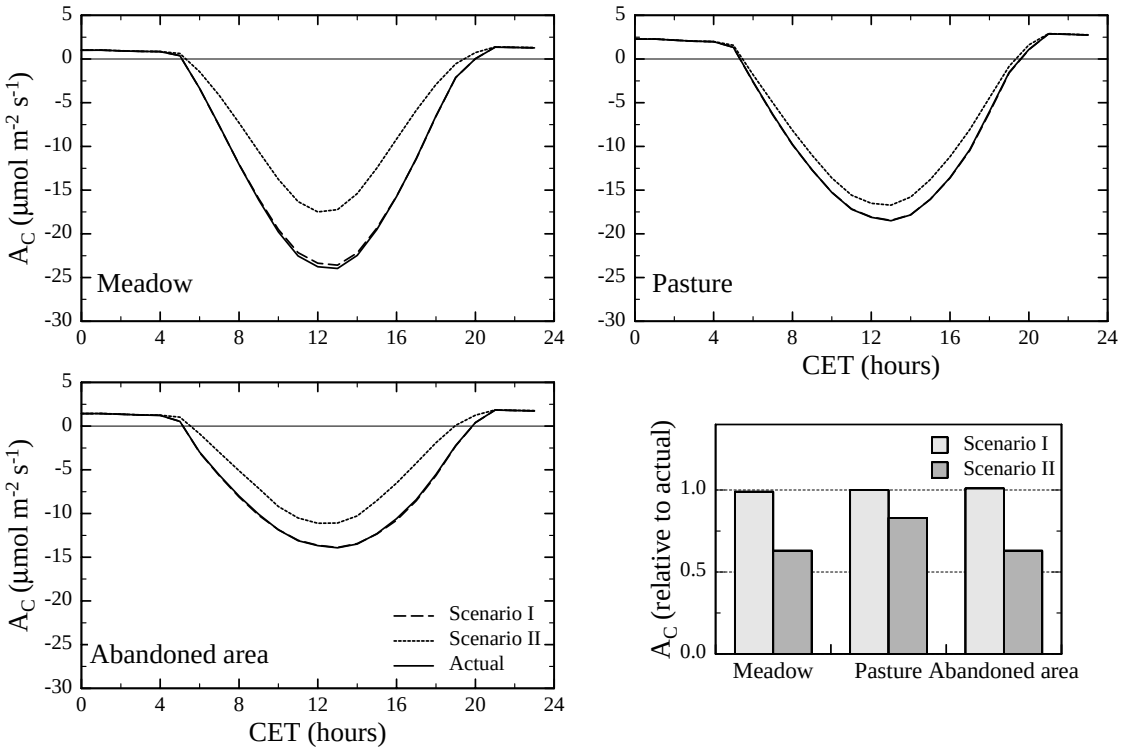

Fig. 7. Simulation experiment investigating the influence of the vertical distribution of the photosynthetically inactive phytomass on canopy net photosynthesis (A_C) for clear sky conditions. Simulations were made with dead plant matter removed from the lowermost canopy layers (Scenario I), and redistributed to the upper third of the canopy (Scenario II). Canopy net photosynthesis is expressed relative to net photosynthesis obtained using unmodified canopy structure (actual) in the bar graph in the lower right corner.

the meadow during any time of the day (Fig. 8B). If we neglect dwarf shrub bole respiration at the abandoned area (hatched areas in Fig. 8), the reduction amounts at solely 10 and 12% for clear and overcast conditions, respectively, i.e. dwarf shrub bole respiration accounts for a reduction in daily net photosynthesis by 4–5%. For comparison, using actual species physiology, net photosynthesis of the pasture and the abandoned area, relative to the meadow, is reduced by 27 and 40% for clear sky conditions, and by 34 and 42% for overcast conditions (Fig. 5).

4. Discussion

Abandonment of mountain meadows and pastures results in a reduction of canopy net photosynthesis relative to their managed state (Tappeiner and Cernusca, 1996, 1998a,b; Tappeiner et al., 1999b). Experimental evidence suggests this decrease to result from associated changes in canopy structure and species physiology (Tappeiner and Cernusca, 1998b). Using a meadow, a pasture and an abandoned area from the Eastern Alps as case studies, the present paper attempts to verify the hypothesised relationships by examining how canopy net photosynthesis is affected by the observed differences in canopy structure and species physiology.

The model reasonably captured the diurnal variation of net photosynthesis at the three investigated sites (Fig. 3), but tended to overestimate daytime net photosynthesis at the meadow, whereas the reverse was true for the pasture and the abandoned area (Table 2). Despite these deficiencies, model calculations account for at least 95% of the variance in measurements, and the mean error is within the range reported by

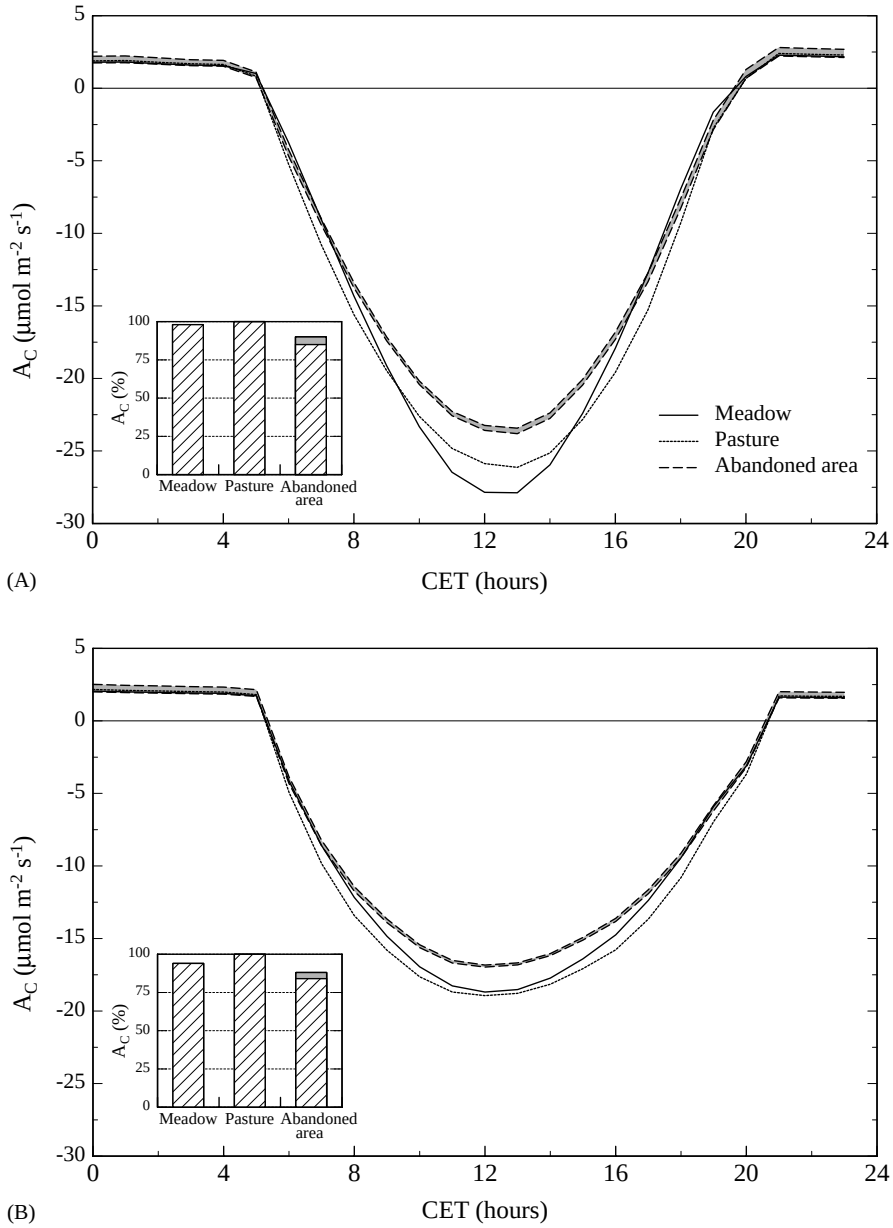

Fig. 8. Simulation experiment investigating the role of canopy structure in determining net photosynthesis (A_C) for clear (A) and overcast (B) sky conditions. Simulations have been conducted assigning the same physiology to the three investigated canopies, while leaving all other parameters unchanged. Simulations for the abandoned area have been made both with and without dwarf shrub respiration losses, the difference is indicated by the grey areas. The insets in the lower right corner show daily net photosynthesis expressed relative to the respective maximum.

other modellers (e.g. Baldocchi and Harley, 1995; Anderson et al., 2000). Employing the present model in a meadow and an abandoned area at the study area Monte Bondone, Wohlfahrt et al. (2001) were able to obtain similar correspondence between measured and simulated canopy net photosynthesis, as well as energy exchange, giving us confidence in both the model and its parameterisation. In addition, the present model has been validated successfully at lower levels of organisation: Wohlfahrt et al. (2000) found good correspondence between measured and simulated leaf net photosynthesis, stomatal conductance and temperature, as well as the attenuation of PPFD and wind speed.

Our modelling analysis suggests that the differences in canopy structure between the three canopies exert a relatively weak influence on canopy net photosynthesis as compared to physiology, which contrasts other studies emphasising a dominating influence of structural features over photosynthetic characteristics (e.g. Barnes et al., 1990; Beyschlag et al., 1990, 1992; Tappeiner and Cernusca, 1998a). Despite the differences between the investigated canopies with regard to canopy height and PAI (Fig. 1, Table 1), it should be noted that the amount of green, photosynthetically active plant matter is fairly similar, varying only between 2.7 and 3.0 $m^2\,m^{-2}$ (Table 1). In fact, Fig. 6 shows that the actual differences with regard to GAI are not large enough to cause the observed differences in net photosynthesis.

This raises the question, why is the amount of photosynthetically inactive phytomass, which in contrast to the GAI varies considerably between the canopies (0.7–2.8 $m^2\,m^{-2}$), of such marginal importance, that in a simulation experiment (Scenario I, Fig. 7) it even may be 'removed' with hardly any effect on canopy net photosynthesis. The key to this question is the vertical position of the photosynthetically inactive phytomass: most of the photosynthetically inactive plant components are located in the lower canopy layers (Fig. 1), being either dead plant parts abscised aloft, senescing phytoelements overtopped by the growing canopy (Miller, 1987) or, in the case of dwarf shrubs, supporting structures (Cernusca, 1976). Deep in the canopy, photosynthesis of the mostly shaded phytoelements is limited by RuBP regeneration most of the day (Baldocchi, 1993; Wohlfahrt et al., 1999b) and thence profits in a linear fashion from an increase in PPFD availability (Farquhar et al., 1980), such as the one brought about by the removal of the photosynthetically inactive plant matter. Yet, for canopy net photosynthesis as a whole the impact is negligible, the fraction of GAI affected by the improved PPFD availability, and thus the increase in net photosynthesis, being too small. In case that appreciable proportions of photosynthetically inactive phytoelements are found in the upper canopy layers (e.g. Tappeiner and Cernusca, 1989, 1998a; Rosset et al., 1999), however, the reverse is the case, as was demonstrated in our modelling experiment by redistributing the removed dead plant material to the upper canopy third (Scenario II, Fig. 7). These findings echo the results of Barnes et al. (1990), who found the sensitivity of net photosynthesis to alterations of structural parameters to be much larger in the upper, than the lower canopy layers.

Net photosynthesis of the investigated canopies scales positively with their bulk photosynthetic capacity, indicating that differences between the canopies with regard to CO_2 uptake are strongly governed by differences in species physiology. The bulk photosynthetic capacities agree well with the results of several studies (Cernusca et al., 1992; Tappeiner and Cernusca, 1998a; Bahn et al., 1999; Wohlfahrt et al., 1999a), who showed that abandoned areas are to a large extent composed by species characterised by low capacities for the biochemical reactions (e.g. dwarf shrubs or the bunch grass *N. stricta*), whereas meadows and pastures are generally made up by graminoids and forbs characterised by high photosynthetic potentials. Following Schulze and Chapin (1987), this is due to the fact that plants have to keep resource use (carbon assimilation, -translocation and -allocation) in balance with resource acquisition (water and nutrient uptake/transport). Abandoned areas, which are characterised by a low nutrient availability (Zeller et al., 2000), thus meet the potentials for carbon assimilation of dwarf shrubs and other species low in photosynthetic capacity more than those of species with high capacities for the biochemical reactions, and vice versa (Wohlfahrt et al., 1999a). In addition, cutting and grazing of meadows and pastures, respectively, prevents dwarf shrubs from establishing at these sites (Tasser et al., 1999).

It is also important to note that net photosynthesis of abandoned areas, as opposed to meadows and

pastures, is not lower merely because of the lower photosynthetic capacities of the dominant species, but also because carbon fixed by photosynthetically active phytoelements is partially lost by dwarf shrub bole respiration (Siegwolf, 1987; Tenhunen et al., 1994). Our model analysis (Fig. 8) suggests that net photosynthesis of the abandoned area is reduced by 4–5% by dwarf shrub bole respiration. Since dwarf shrubs, as opposed to herbaceous species, are slow growing species (Schulze, 1982; Schulze and Chapin, 1987), dwarf shrub bole respiration is likely to gain increasing importance for the carbon balance with the duration of abandonment, during which dwarf shrubs usually increase in fractional cover (Tasser et al., 1999).

5. Conclusion

By means of a model analysis, this paper shows that net photosynthesis of the investigated canopies is directly related to their bulk photosynthetic capacity, indicating a prominent influence of species physiology. Differences in canopy structure, on the other hand, are of minor importance for net photosynthesis. This is because green area is too similar to be a major source of variation in net photosynthesis. In addition, photosynthetically inactive phytoelements, whose amount varies considerably between the investigated canopies, exert little influence on canopy net photosynthesis, since most of them are accumulated close to the ground surface. These results, however, must not be generalised, since it was also found that photosynthetically inactive phytoelements may cause appreciable reductions in net photosynthesis in case they constitute comparably large proportions of the upper canopy layers.

Future work should now be directed towards incorporating soil and off-site carbon losses into the present model and at integrating model simulations over the annual cycle (cf. Baldocchi and Wilson, 2001), in order to gain a full picture of how land use affects the carbon balance of the investigated ecosystems.

Acknowledgements

This study was conducted within the EU-TERI-project ECOMONT (project no. ENV4-CT95-0179) and the FWF-project P13963-BIO (Austrian National Science Foundation). We are indebted to Elke Haubner, Ingrid Horak, Piero Nalin, Walter Michaeler, Karin Rottmar and Marco Zucchelli for their assistance with field work.

Appendix A. Model theory and parameterisation

A.1. Leaf gas exchange

Following Farquhar et al. (1980) and Farquhar and Von Caemmerer (1982) CO_2 assimilation is either entirely limited by the kinetic properties of RUBISCO and the respective concentrations of the competing gases CO_2 and O_2 at the sites of carboxylation (W_C) or by electron transport (W_J), which limits the rate at which RuBP is regenerated. Net photosynthesis A ($\mu mol\,m^{-2}\,s^{-1}$) may then be expressed as

$$A = \left(1 - \frac{0.5 O_i}{\tau C_i}\right) \min\{W_C, W_J\} - R_{day}, \qquad (A.1)$$

where O_i and C_i are the concentrations of O_2 ($mmol\,mol^{-1}$) and CO_2 ($\mu mol\,mol^{-1}$) in the intercellular space, respectively, τ is the specificity factor for RUBISCO, R_{day} is the rate of CO_2 evolution from processes other than photorespiration ($\mu mol\,m^{-2}\,s^{-1}$) and $\min\{\cdot\}$ denotes 'the minimum of'.

To be able to predict gas exchange at the leaf level, the photosynthesis model has to be combined with a model predicting stomatal conductance. For this purpose the empirical model by Ball et al. (1987), including the modifications by Falge et al. (1996), was chosen

$$g_{sv} = g_{min} + G_{fac}(A + I_{fac} R_{dark}) 10^3 \frac{h_s}{C_s}, \qquad (A.2)$$

where g_{sv} is the stomatal conductance ($mmol\,m^{-2}\,s^{-1}$), g_{min} is the minimum or residual stomatal conductance ($mmol\,m^{-2}\,s^{-1}$) and h_s and C_s are the relative humidity and the CO_2 concentration ($\mu mol\,mol^{-1}$) at the leaf surface. G_{fac} is an empirical coefficient representing the composite sensitivity of stomata to these factors. R_{dark} is the dark respiration ($\mu mol\,m^{-2}\,s^{-1}$) and I_{fac} represents the extent to which dark respiration is inhibited in the light.

Leaf internal CO_2 concentration is calculated from net photosynthesis and stomatal conductance accord-

ing to Fick's law:

$$C_i = C_s - \frac{A \times 1600}{g_{sv}}, \quad (A.3)$$

where 1600 accounts for the difference in diffusivity between CO_2 and H_2O and corrects for the difference in the units of A and g_{sv}.

As A, g_{sv} and C_i are dependent, the above equations must be solved in an iterative fashion. An analytical solution exists only if h_s in Eq. (A.2) is assumed to equal free air relative humidity (Baldocchi, 1994). This simplification was circumvented in the present approach by embedding the analytical solution of Baldocchi (1994) into a single iteration loop for h_s, which is straightforward.

Leaf model parameters of the investigated species were determined from leaf gas exchange measurements, as detailed in Wohlfahrt et al. (1998), and are shown in Table A.1. Model parameters of the generic components (Table A.2) were derived from a survey of 30 mountain grassland species by Wohlfahrt et al. (1999a), as described in Wohlfahrt et al. (2001).

A.2. Bole respiration

An Arrhenius-type equation is used to model respiration of woody stems as a function of temperature:

$$R_{bole} = R_{bole}(T_{ref}) \exp\left[\frac{\Delta H_a}{R T_{ref}}\left(1 - \frac{T_{ref}}{T_{pK}}\right)\right], \quad (A.4)$$

where $R_{bole}(T_{ref})$ is the respiration rate ($\mu mol\,m^{-2}\,s^{-1}$) at the reference temperature (T_{ref}, 273.16 K), T_{pK} is the absolute temperature (K), R is the universal gas constant ($8.314\,J\,mol^{-1}\,K^{-1}$) and ΔH_a is an activation energy ($J\,mol^{-1}$).

Parameters describing bole respiration of green and non-green stems of dwarf shrubs were derived from gas exchange measurements on *Rhododendron ferrugineum* by Siegwolf (1987), as described in Wohlfahrt et al. (2001).

A.3. The energy balance

Phytoelement surface temperatures are estimated solving their energy balance equation:

$$R_{abs} = L_e + L_E + H = 2\varepsilon_c \sigma T_{pK}^4 + \frac{\rho c_p}{\gamma}[e_s(T_p) - e_{air}]g_{tv} + \rho c_p (T_p - T_{air})\frac{g_{bv}}{Lw^x}, \quad (A.5)$$

where R_{abs} is the bi-directional absorbed short- and long-wave radiation, L_e is the emitted long-wave radiation, L_E and H represent latent and sensible heat exchange, respectively (all $W\,m^{-2}$), ε_c is the phytoelement thermal emissivity, σ is the Stefan–Boltzmann constant ($5.67 \times 10^{-8}\,W\,m^{-2}\,K^{-4}$), ρ and c_p are the density ($kg\,m^{-3}$) and the specific heat ($1010\,J\,kg^{-1}\,K^{-1}$) of dry air, respectively, γ is the psychrometric constant ($Pa\,K^{-1}$), $e_s(T_p)$ is the saturated leaf water vapour pressure (hPa) at the phytoelement temperature T_p (°C), e_{air} is the air–water vapour pressure (hPa), T_{air} is the air temperature (°C) and g_{tv} is the total conductance to water vapour ($mmol\,m^{-2}\,s^{-1}$). The calculation of g_{tv} depends on whether water is present on the phytoelement surfaces or not. In the absence of surface water, g_{tv} is calculated as

$$g_{tv} = \frac{g_{sv} g_{bv} \delta}{g_{sv} + g_{bv}\delta}, \quad (A.6)$$

where g_{bv} is the all-sided boundary layer conductance to water vapour ($mmol\,m^{-2}\,s^{-1}$) and δ is a Boolean variable indicating whether leaves have stomata on one ($\delta = 0.5$) or both ($\delta = 1$) leaf sides. Leaves are treated as hypostomatous, green stems as amphistomatous. If phytoelements are wet (either due to dew formation, or the interception of precipitation or dew), g_{tv} reduces to g_{bv} (Nikolov et al., 1995). Dew forms on a phytoelement surface if the surface temperature drops below the dew point temperature of the surrounding air. The calculations of dew dynamics recognise that phytoelements hold water up to a maximum capacity before the onset of dripping to the canopy components below, following an approach described in Wilson et al. (1999).

Boundary layer conductances to water vapour are modelled making use of the non-dimensional groups, depending on whether forced or free convection prevails. In order to account for the enhancement of boundary layer conductances due to the turbulent nature of outdoor environments a factor of 1.4 is included (Campbell and Norman, 1998). The boundary layer conductance to water vapour is converted to that to heat by g_{bv}/Lw^x, where Lw is the Lewis number and x takes $-2/3$ and $-3/4$, respectively, for forced and free convection. The energy balance algorithm is solved in an analytical fashion following Nikolov et al. (1995).

Table A.1
Parameters of the combined leaf photosynthesis and stomatal conductance model of the investigated key-species

Parameter	Units	Acmi	Alvu[a]	Armo	Cavu	Nast	Plme	Poau	Rhal	Rual	Treu	Trmo	Trpr	Trre	Vamy
$V_{C\,max}$															
$V_{C\,max}$ (T_{ref})	μmol m^{-2} s^{-1}	63.67	20.47	28.96	16.39	12.25	57.53	30.03	53.24	47.32	35.07	56.67	48.79	71.25	13.30
ΔH_a ($V_{C\,max}$)	J mol^{-1}	109740	57719	54726	102570	61304	51300	57098	60600	83300	68000	118599	53017	56796	102568
ΔH_d ($V_{C\,max}$)	J mol^{-1}	199500	202133	201500	200000	202583	200000	204000	202000	200000	201000	197500	202000	202000	201194
P_{ml}															
P_{ml} (T_{ref})	μmol m^{-2} s^{-1}	29.93	10.10	18.62	10.67	5.93	35.71	17.48	26.71	26.12	22.93	35.38	27.03	43.10	5.57
ΔH_a (P_{ml})	J mol^{-1}	41052	57002	55973	57330	44386	43594	57101	37407	89742	55465	115191	68707	44281	57329
ΔH_d (P_{ml})	J mol^{-1}	199400	196000	197000	197100	196168	196200	199247	201000	196268	199521	191300	199000	196000	198922
R_{dark}															
R_{dark} (T_{ref})	μmol m^{-2} s^{-1}	2.95[a]	1.31	1.32[a]	0.44[a]	0.84[a]	2.94[a]	0.68	1.47	1.52[a]	1.24	2.16	0.80	1.72[a]	1.31
ΔH_a (R_{dark})	J mol^{-1}	39654[a]	34936	56227[a]	95795[a]	52013[a]	33004[a]	94482	70418	47330[a]	36743	43432	40479	58447[a]	22821
α	mol CO_2 mol photons^{-1}	0.065[a]	0.06	0.06[a]	0.06[a]	0.05[a]	0.06[a]	0.06	0.06	0.06[a]	0.06	0.06	0.06	0.065[a]	0.06
G_{fac}	–	5.3[a]	11.9	9.4[a]	15.4[a]	8.6[a]	11.3[a]	24.7	18.3	6.7[a]	13.4	13.5	6.9	6.9[a]	10.5
g_{min}	mmol m^{-2} s^{-1}	158.8[a]	97.2	71.6[a]	59.7[a]	57.8[a]	122.3[a]	130.0	193.1	78.3[a]	67.0	42.6	25.2	45.8[a]	11.7
A_{max}[b]	μmol m^{-2} s^{-1}	15.2	12.1	7.6	4.7	3.3	14.9	8.2	15.7	11.5	9.5	14.0	11.1	16.3	3.2

A. millefolium (Acmi), *A. vulgaris* (Alvu), *A. montana* (Armo), *C. vulgaris* (Cavu), *N. stricta* (Nast), *P. media* (Plme), *P. aurea* (Poau), *R. alectorolophus* (Rhal), *R. alpestris* (Rual), *T. europaeus* (Treu), *T. montanum* (Trmo), *T. pratense* (Trpr), *T. repens* (Trre) and *V. myrtillus* (Vamy). $\Delta S(V_{C\,max})$ and $\Delta S(P_{ml})$ were fixed for all species at 656 and 643 J K^{-1} mol^{-1}, respectively (cf. Wohlfahrt et al., 1998). $V_{C\,max}$ is the maximum rate of carboxylation, P_{ml} is the potential rate of RuBP regeneration, A_{max} is the photosynthetic capacity and α is the apparent quantum yield at saturating CO_2. For other symbols refer to Appendix A. Data are from Wohlfahrt et al. (1998, 1999a), except for: [a]Wohlfahrt et al., unpublished; [b]Bahn et al. (1999).

Table A.2
Parameters of the combined photosynthesis and stomatal conductance model for leaves and stems of forbs (FL and FS, respectively) and graminoids (GL and GS, respectively) at the investigated sites

Parameter	Units	Meadow		Pasture		Abandoned area	
		FL, FS	GL, GS	FL, FS	GL, GS	FL, FS	GL, GS
$V_{C\,max}$							
$V_{C\,max}$ (T_{ref})	$\mu mol\,m^{-2}\,s^{-1}$	53.52	39.41	45.78	30.21	35.86	36.24
ΔH_a ($V_{C\,max}$)	$J\,mol^{-1}$	69752	87624	70296	131966	69022	55125
ΔH_d ($V_{C\,max}$)	$J\,mol^{-1}$	200652	198801	200870	198603	200336	201578
P_{ml}							
P_{ml} (T_{ref})	$\mu mol\,m^{-2}\,s^{-1}$	28.73	22.21	25.52	17.98	21.21	23.66
ΔH_a (P_{ml})	$J\,mol^{-1}$	48840	75926	54135	55488	52710	46270
ΔH_d (P_{ml})	$J\,mol^{-1}$	198190	194482	197265	200141	197095	196019
R_{dark}							
R_{dark} (T_{ref})	$\mu mol\,m^{-2}\,s^{-1}$	1.52	0.94	2.30[b]	1.52[b]	1.56	1.46
ΔH_a (R_{dark})	$J\,mol^{-1}$	48966	93544	45276[b]	83890[b]	51628	49942
α[a]	mol CO_2 mol photons^{-1}	0.055	0.055	0.055	0.055	0.055	0.055
G_{fac}	–	14.4	15.4	11.3[b]	13.0[b]	9.7[b]	8.6[b]
g_{min}	$mmol\,m^{-2}\,s^{-1}$	80.3	75.8	122.3[b]	10.2[b]	60.0[b]	57.8[b]
A_{max}[b]	$\mu mol\,m^{-2}\,s^{-1}$	13.4	14.2	12.0	7.6	9.0	9.3

$\Delta S(V_{C\,max})$ and $\Delta S(P_{ml})$ were fixed for all components at 656 and 643 $J\,K^{-1}\,mol^{-1}$, respectively (cf. Wohlfahrt et al., 1998). $V_{C\,max}$ is the maximum rate of carboxylation, P_{ml} is the potential rate of RuBP regeneration, A_{max} is the photosynthetic capacity and α is the apparent quantum yield at saturating CO_2. For other symbols refer to Appendix A. Parameters are from Wohlfahrt et al. (1999a, 2001), except for: [a]Baldocchi and Meyers (1998); [b]Wohlfahrt et al., unpublished.

A.4. Within-canopy profiles of wind speed, CO_2 and H_2O concentration, and air temperature

A logarithmic equation is used to model wind speed in the sparse, upper canopy layers down to the upper height of the thick lower canopy layers, below which attenuation proceeds exponentially (Wohlfahrt et al., 2000). A simple half-order closure scheme is adopted for the concentration profiles of CO_2 and H_2O, i.e. they are assumed to be constant within the canopy, which yields only small errors in the computation of CO_2 and latent heat fluxes (Baldocchi, 1992). Sensible heat exchange, on the other hand, depends strongly on the within-canopy air temperature profile (Baldocchi, 1992), which in the present approach is pre-described using measured profiles of within-canopy air temperature.

A.5. Radiative transfer

The model of radiative transfer treats the canopy as a horizontally homogeneous, plane-parallel turbid medium in which multiple scattering occurs on the elements of turbidity (phytoelements) of the different components, each having their own optical and geometrical properties. The canopy is divided into sufficiently small (0.1 $m^2\,m^{-2}$), statistically independent layers, within which self-shading may be considered negligible and phytoelements to be distributed symmetrically with respect to the azimuth. Hemispherical reflection and transmission of radiation, which are allowed to be unequal, are assumed to be lambertian. Nine inclination classes are considered.

Assuming that phytoelements are distributed at random, the probability that a ray of light incident at an angle (from the horizontal) β is intercepted in a layer j (counted from bottom upwards) by the phytoelements of a component p with a hemi-surface area of ΔL ($m^2\,m^{-2}$) and inclined as described by a inclination distribution F, is given by (Goudriaan, 1977):

$$P(p, j, \beta) = \frac{\Delta L(p, j)}{\sin\beta} \sum_{\lambda=1}^{9} F(p, j, \lambda) G(p, j, \beta, \lambda), \tag{A.7}$$

where G is the projection of the phytoelements inclined at an angle λ into the direction β.

The radiation distribution within the canopy is bi-modal. Shaded phytoelements receive diffuse light only, while sunlit ones receive both diffuse and direct radiation, the latter incident at an angle β^*, the elevation of the sun. The attenuation of beam radiation (Q_{dir}) is calculated as

$$Q_{\mathrm{dir}}(j) = Q_{\mathrm{dir}}(j+1) - \sum_{p=1}^{np} Q_{\mathrm{dir}}(j+1)\,P(p, j, \beta^*), \tag{A.8}$$

where *np* stands for the number of phytoelements. The fraction of sunlit phytoelement area is proportional to the attenuation of direct radiation.

The flux of diffuse radiation in the canopy consists of diffuse radiation from the atmosphere and of diffused, scattered beam radiation. For the treatment of diffuse radiation, the upper and lower hemispheres viewed by the phytoelements are divided into nine sectors of 10° each. The downward and upward diffuse short-wave fluxes within the canopy consist of the non-intercepted diffuse radiation from above and below, respectively, the diffuse radiation transmitted from above and reflected from below downwards and vice versa, and the direct radiation transmitted in the downward and reflected in the upward direction, respectively. The downward and upward fluxes of long-wave radiation consist of the non-intercepted flux from above and below, respectively, the upward radiation reflected downwards and the downward radiation reflected upwards, respectively, and the emitted radiation. The latter is calculated as the weighted mean flux from sunlit and shaded phytoelements. At the soil surface radiation is assumed to be reflected/emitted lambertian.

Vegetation and soil optical properties were borrowed from various literature sources, as detailed in Wohlfahrt et al. (2001). Solar elevation is calculated using the equations given in Campbell and Norman (1998). Partitioning of solar radiation into PPFD and near infrared components is modelled using the approach described in Goudriaan (1977).

References

Anderson, M.C., Norman, J.M., Meyers, T.P., Diak, G.R., 2000. An analytical model for estimating canopy transpiration and carbon assimilation fluxes based on canopy light-use efficiency. Agric. For. Meteorol. 101, 265–289.

Bahn, M., Cernusca, A., Tappeiner, U., Tasser, E., 1994. Wachstum krautiger Arten auf einer Mähwiese und einer Almbrache. Ver. Ges. Ökol. 23, 23–30.

Bahn, M., Wohlfahrt, G., Haubner, E., Horak, I., Michaeler, W., Rottmar, K., Tappeiner, U., Cernusca, A., 1999. Leaf photosynthesis, nitrogen contents and specific leaf area of grassland species in mountain ecosystems under different land use. In: Cernusca, A., Tappeiner, U., Bayfield, N. (Eds.), Land-Use Changes in European Mountain Ecosystems. ECOMONT—Concepts and Results. Blackwell Wissenschafts-Verlag, Berlin, pp. 247–255.

Baldocchi, D.D., 1992. A Lagrangian random walk model for simulating water vapor, CO_2 and sensible heat flux densities and scalar profiles over and within a soybean canopy. Boundary Layer Meteorol. 61, 113–144.

Baldocchi, D.D., 1993. Scaling water vapour and carbon dioxide exchange from leaves to canopy: rules and tools. In: Ehleringer, J.R., Field, C.B. (Eds.), Scaling Physiological Processes: Leaf to Globe. Academic Press, San Diego, pp. 77–116.

Baldocchi, D.D., 1994. An analytical solution for coupled leaf photosynthesis and stomatal conductance models. Tree Physiol. 14, 1069–1079.

Baldocchi, D.D., Harley, P.C., 1995. Scaling carbon dioxide and water vapor exchange from leaf to canopy in a deciduous forest. II. Model testing and application. Plant Cell Environ. 18, 1157–1173.

Baldocchi, D.D., Meyers, T., 1998. On using eco-physiological, micrometeorological and biogeochemical theory to evaluate carbon dioxide, water vapor and trace gas fluxes over vegetation: a perspective. Agric. For. Meteorol. 90, 1–25.

Baldocchi, D.D., Wilson, K.B., 2001. Modelling CO_2 and water vapor exchange of a temperate broadleaved forest across hourly to decadal time scales. Ecol. Model. 142, 155–184.

Ball, J.T., Woodrow, I.E., Berry, J.A., 1987. A model predicting stomatal conductance and its contribution to the control of photosynthesis under different environmental conditions. In: Biggens, J. (Ed.), Progress in Photosynthesis Research, Proceedings of the VII International Congress on Photosynthesis, vol. IV. Martinus Nijhoff, Dordrecht, pp. 221–224.

Barnes, P.W., Beyschlag, W., Ryel, R., Flint, S.D., Caldwell, M.M., 1990. Plant competition for light analyzed with a multispecies canopy model III. Influence of canopy structure in mixtures and monocultures of wheat and wild oat. Oecologia 82, 560–566.

Beyschlag, W., Barnes, P.W., Ryel, R., Caldwell, M.M., Flint, S.D., 1990. Plant competition for light analyzed with a multispecies canopy model. II. Influence of photosynthetic characteristics on mixtures of wheat and wild oat. Oecologia 82, 374–380.

Beyschlag, W., Ryel, R.J., Ullman, I., 1992. Experimental and modelling studies of competition for light in roadside grasses. Bot. Acta 105, 285–291.

Bitterlich, W., Cernusca, A., 1999. Stubai Valley composite landscape, Tyrol, Austria. In: Cernusca, A., Tappeiner, U., Bayfield, N. (Eds.), Land-Use Changes in European Mountain Ecosystems. ECOMONT—Concepts and Results. Blackwell Wissenschafts-Verlag, Berlin, pp. 35–45.

Campbell, G.S., Norman, J.M., 1998. An Introduction to Environmental Biophysics. Springer Verlag, New York, 286 pp.

Cernusca, A., 1976. Bestandesstruktur, bioklima und energiehaushalt von Alpine zwergstrauchbeständen. Oecologia Plant. 11, 71–102.

Cernusca, A., 1987. Application of computer methods in the field to assess ecosystem function and response to stress. In: Tenhunen, J.D., Catarino, F.M., Lange, O.L., Oechel, W.C. (Eds.), Plant Response to Stress, NATO ASI Series, vol. G15. Springer Verlag, Berlin, pp. 157–164.

Cernusca, A., Tappeiner, U., Agostini, A., Bahn, M., Bezzi, A., Egger, R., Kofler, R., Newesely, Ch., Orlandi, D., Prock, S., Schatz, H., Schatz, I., 1992. Ecosystem research on mixed grassland/woodland ecosystems. First results of the EC-STEP-project INTEGRALP on Mt. Bondone Stud. Trent. Sci. Nat. Acta Biol. 67, 99–133.

Cernusca, A., Tappeiner, U., Bahn, M., Bayfield, N., Chemini, C., Fillat, F., Graber, W., Rosset, M., Siegwolf, R., Tenhunen, J., 1996. ECOMONT—ecological effects of land-use changes on european terrestrial mountain ecosystems. Pirineos 147/148, 145–172.

Cernusca, A., Bahn, M., Chemini, C., Graber, W., Siegwolf, R., Tappeiner, U., Tenhunen, J., 1998a. ECOMONT: a combined approach of field measurements and process-based modelling for assessing effects of land-use changes in mountain landscapes. Ecol. Model. 113, 167–178.

Cernusca, A., Bahn, M., Bayfield, N., Chemini, C., Fillat, F., Graber, W., Rosset, M., Siegwolf, R., Tappeiner, U., Tasser, E., Tenhunen, J., 1998b. ECOMONT: new concepts for assessing ecological effects of land use changes on terrestrial mountain ecosystems at a European scale. Ver. Ges. Ökol. 28, 3–11.

Cernusca, A., Tappeiner, U., Bayfield, N., 1999. Land-Use Changes in European Mountain Ecosystems. ECOMONT—Concepts and Results. Blackwell Wissenschaftsverlag, Berlin, 368 pp.

Cescatti, A., Chemini, C., De Siena, C., Gianelle, D., Nicolini, G., Wohlfahrt, G., 1999. Monte Bondone composite landscape, Italy. In: Cernusca, A., Tappeiner, U., Bayfield, N. (Eds.), Land-Use Changes in European Mountain Ecosystems. ECOMONT—Concepts and Results. Blackwell Wissenschafts-Verlag, Berlin, pp. 60–73.

Evans, J.R., 1989. Photosynthesis and nitrogen relationships in leaves of C_3 plants. Oecologia 78, 9–19.

Falge, E., Graber, W., Siegwolf, R., Tenhunen, J.D., 1996. A model of the gas exchange of *Picea abies* to habitat conditions. Trees 10, 277–287.

Farquhar, G.D., Von Caemmerer, S., 1982. Modelling of photosynthetic response to environmental conditions. In: Lange, O.L., Nobel, P.S., Osmond, C.B., Ziegler, H. (Eds.), Physiological Plant Ecology. Encyclopaedia of Plant Physiology 12B, vol. II. Springer Verlag, Berlin, pp. 549–588.

Farquhar, G.D., Von Caemmerer, S., Berry, J.A., 1980. A biochemical model of photosynthetic CO_2 assimilation in leaves of C_3 species. Planta 149, 78–90.

Field, C., Mooney, H.A., 1986. The photosynthesis–nitrogen relationship in wild plants. In: Givinish, T.J. (Ed.), On the Economy of Plant Form and Function. Cambridge University Press, Cambridge, pp. 25–55.

Fox, A.D., Kristiansen, J.N., Stroud, D.A., Boyd, H., 1998. The effects of simulated spring goose grazing on the growth rate and protein content of *Phleum pratense* leaves. Oecologia 116, 154–159.

Goudriaan, J., 1977. Crop Micrometeorology: A Simulation Study. Pudoc, Wageningen, 249 pp.

Houghton, R.A., 1995. Land-use change and the carbon cycle. Global Change Biol. 1, 275–287.

Houghton, R.A., 1999. The annual net flux of carbon to the atmosphere from changes in land use 1850–1990. Tellus 51B, 298–313.

Intergovernmental Panel on Climate Change, 2000. Special Report on Land Use, Land Use Change, and Forestry. ISBN 92-9169-114-3.

Lentz, K.A., Cipollini, D.F., 1998. Effect of light and simulated herbivory on growth of endangered north-eastern bulrush, *Scirpus ancistrochaetus* Schuyler. Plant Ecol. 139, 125–131.

Leuning, R., Kelliher, F.M., De Pury, D.G.G., Schulze, E.D., 1995. Leaf nitrogen, photosynthesis, conductance and transpiration: scaling from leaves to canopies. Plant Cell Environ. 18, 1183–1200.

Lloyd, J., 1999. Current perspectives on the terrestrial carbon cycle. Tellus 51B, 336–342.

Miller, T.E., 1987. Effects of emergence time on survival and growth in an early old-field plant community. Oecologia 72, 272–278.

Nikolov, N.T., Massman, W.J., Schoettle, A.W., 1995. Coupling biochemical and biophysical processes at the leaf level: an equilibrium photosynthesis model for leaves of C_3 plants. Ecol. Model. 80, 205–235.

Paldele, B., 1994. Die Aufgelassenen Almen Tirols. Innsbrucker Geographische Studien Bd. 23, Institut für Geographie der Universität Innsbruck, Innsbruck.

Perez, P.J., Castellvi, F., Ibanez, M., Rosell, J.I., 1999. Assessment of reliability of Bowen ratio method for partitioning of fluxes. Agric. For. Meteorol. 97, 141–150.

Reich, P.B., Kloeppel, B.D., Ellsworth, D.S., Walters, M.B., 1995. Different photosynthesis–nitrogen relations in deciduous hardwood and evergreen coniferous tree species. Oecologia 104, 24–30.

Rosset, M., Gerber, N., Tanner, M., Fuhrer, J., 1999. Canopy structure, radiation balance and evapotranspiration in managed and abandoned hay meadows at Rotenbach, Switzerland. In: Cernusca, A., Tappeiner, U., Bayfield, N. (Eds.), Land-Use Changes in European Mountain Ecosystems. ECOMONT—Concepts and Results. Blackwell Wissenschafts-Verlag, Berlin, pp. 280–288.

Schulze, E.D., 1982. Plant life forms and their carbon, water and nutrient relations. In: Lange, O.L., Nobel, P.S., Osmond, C.B., Ziegler, H. (Eds.), Physiological Plant Ecology. Encyclopedia of Plant Physiology 12B, vol. II. Springer Verlag, Berlin, pp. 615–676.

Schulze, E.D., Chapin III, F.S., 1987. Plant specialisation to environments of different resource availability. In: Schulze, E.D., Zwölfer, H. (Eds.), Potentials and Limitations to Ecosystem Analysis, Ecological Studies, vol. 61. Springer Verlag, Berlin, pp. 120–147.

Siegwolf, R., 1987. CO_2-Gaswechsel von *Rhododendron ferrugineum* L. im Jahresgang an der Alpinen Waldgrenze. Ph.D. Thesis, University of Innsbruck, 283 pp.

Smith, P., Powlson, D.S., Smith, J.U., Falloon, P., Coleman, K., 2000. Meeting Europe's climate change commitments: quantitative estimates of the potential for carbon mitigation by agriculture. Global Change Biol. 6, 525–539.

Spatz, G., Fricke, T., Prock, S., 1993. Wirtschaftsbedingte vegetationsmuster auf almweiden der hohen tauern. Revue de Gèographie Alpine 3, 83–93.

Steffen, W., Noble, I., Canadell, J., Apps, M., Schulze, E.-D., Jarvis, P.G., Baldocchi, D., Ciais, P., Cramer, W., Ehleringer, J., Farquhar, G., Field, C.B., Ghazi, A., Gifford, R., Heimann, M., Houghton, R., Kabat, P., Körner, Ch., Lambin, E., Linder, S., Mooney, H.A., Murdiyarso, D., Post, W.M., Prentice, C., Raupach, M.R., Schimel, D.S., Shvidenko, A., Valentini, R., 1998. The terrestrial carbon cycle: implications for the Kyoto protocol. Science 280, 1393–1394.

Tappeiner, U., Cernusca, A., 1989. Veränderung der Bestandesstruktur und der Lichtausnützung nach dem Brachfallen einer Almweide. In: Cernusca, A. (Ed.), Struktur und Funktion von Graslandökosystemen im Nationalpark Hohe Tauern. Veröffentlichungen des österreichischen MaB-Programms, Band 13, Wagner, Innsbruck, pp. 531–547.

Tappeiner, U., Cernusca, A., 1994. Bestandesstruktur, energiehaushalt und bodenatmung einer mähwiese, einer almweide und einer almbrache. Ver. Ges. Ökol. 23, 49–56.

Tappeiner, U., Cernusca, A., 1996. Microclimate and fluxes of water vapour, sensible heat and carbon dioxide in structurally differing subalpine plant communities in the Central Caucasus. Plant Cell Environ. 19, 403–417.

Tappeiner, U., Cernusca, A., 1998a. Model simulation of spatial distribution of photosynthesis in structurally differing plant communities in the Central Caucasus. Ecol. Model. 113, 201–223.

Tappeiner, U., Cernusca, A., 1998b. Effects of land-use changes in the Alps on exchange processes (CO_2, H_2O) in grassland ecosystems. In: Proceedings of the HeadWater'98 Conference on Hydrology, Water Resources and Ecology in Headwaters, Meran/Merano, Italy, April 1998. IAHS Publication No. 248, pp. 131–138.

Tappeiner, U., Tasser, E., Mayr, V., Ostendorf, B., 1999a. Passeier Valley Composite Landscape, Italy. In: Cernusca, A., Tappeiner, U., Bayfield, N. (Eds.), Land-Use Changes in European Mountain Ecosystems. ECOMONT—Concepts and Results. Blackwell Wissenschafts-Verlag, Berlin, pp. 46–59.

Tappeiner, U., Cernusca, A., Siegwolf, R.T.W., Sapinsky, S., Newesely, Ch., Geissbühler, P., Stefanicki, G., 1999b. Microclimate, energy budget and CO_2 gas exchange of ecosystems. In: Cernusca, A., Tappeiner, U., Bayfield, N. (Eds.), Land-Use Changes in European Mountain Ecosystems. ECOMONT—Concepts and Results. Blackwell Wissenschafts-Verlag, Berlin, pp. 135–145.

Tasser, E., Prock, S., Mulser, J., 1999. Impact of land use on vegetation along the Eastern Alpine transect. In: Cernusca, A., Tappeiner, U., Bayfield, N. (Eds.), Land-Use Changes in European Mountain Ecosystems. ECOMONT—Concepts and Results. Blackwell Wissenschafts-Verlag, Berlin, pp. 235–246.

Tenhunen, J.D., Siegwolf, R.T.W., Oberbauer, S.F., 1994. Effects of phenology, physiology, and gradients in community composition, structure, and microclimate on tundra ecosystem CO_2 exchange. In: Schulze, E.-D., Caldwell, M.M. (Eds.), Ecophysiology of Photosynthesis. Ecological Studies, vol. 100. Springer Verlag, Heidelberg, pp. 431–458.

Valentini, R., Dolman, H., Ciais, P., Schulze, E.-D., Freibauer, A., Schimel, D., Heimann, M., 2000. Accounting for Carbon Sinks in the Biosphere, European Perspective. CARBOEUROPE European Office, Max-Planck-Institute for Biogeochemistry, Jena, Germany, 15 pp.

Wilson, T.B., Bland, W.L., Norman, J.M., 1999. Measurement and simulation of dew accumulation and drying in a potato canopy. Agric. For. Meteorol. 93, 111–119.

Wohlfahrt, G., Bahn, M., Horak, I., Tappeiner, U., Cernusca, A., 1998. A nitrogen sensitive model of leaf carbon dioxide and water vapour gas exchange: application to 13 key species from differently managed mountain grassland ecosystems. Ecol. Model. 113, 179–199.

Wohlfahrt, G., Bahn, M., Haubner, E., Horak, I., Michaeler, W., Rottmar, K., Tappeiner, U., Cernusca, A., 1999a. Inter-specific variation of the biochemical limitation to photosynthesis and related leaf traits of 30 species from mountain grassland differing in land use. Plant Cell Environ. 22, 1281–1296.

Wohlfahrt, G., Bahn, M., Cernusca, A., 1999b. The use of the ratio between the photosynthesis parameters P_{ml} and V_{Cmax} for scaling up photosynthesis of C_3 plants from leaves to canopies: a critical examination of different modelling approaches. J. Theor. Biol. 200, 163–181.

Wohlfahrt, G., Bahn, M., Tappeiner, U., Cernusca, A., 2000. A model of whole plant gas exchange for herbaceous species from mountain grassland sites differing in land use. Ecol. Model. 125, 173–201.

Wohlfahrt, G., Bahn, M., Tappeiner, U., Cernusca, A., 2001. A multi-component, multi-species model of vegetation–atmosphere CO_2 and energy exchange for mountain grasslands. Agric. For. Meteorol. 106, 261–287.

Zeller, V., Bahn, M., Aichner, M., Tappeiner, U., 2000. Impact of land-use change on nitrogen mineralisation in subalpine grasslands in the Eastern Alps. Biol. Fertil. Soils 31, 441–448.